Predicting IFN-γ responses after BCG vaccination in humans from macaques: A proof-of-concept study of Immunostimulation/ Immunodynamic modelling methods

Running title: **Predicting BCG IFN-γ responses in humans from macaques**

Authors: Sophie J Rhodes*[a#], Charlotte Sarfas*[b], Gwenan M Knight[a,c], Andrew White[b], Ansar A. Pathan[d], Helen McShane[e], Thomas G. Evans[f], Helen Fletcher[g], Sally Sharpe**[b], Richard G White**[a]

[a] TB Modelling Group, CMMID, TB Centre, London School of Hygiene and Tropical Medicine, UK

[b] Public Health England, Porton down, UK

[c] Imperial College, London, UK

[d] College of Health and Life Sciences, Department of Life Sciences, Brunel University, UK

[e] The Jenner Institute, University of Oxford, UK

[f] TomegaVax, Portland Oregon, USA

[g] Immunology and Infection Department, London School of Hygiene and Tropical Medicine, UK

Address correspondence to Sophie Rhodes, Sophie.rhodes@lshtm.ac.uk

*Joint first author

**Joint senior author

Abstract

Introduction: Macaques play a central role in human tuberculosis(TB) vaccine development. Immune and challenge responses differ across macaque and human subpopulations. We determined which macaque subpopulations best predicted immune responses in different human subpopulations, using novel immunostimulation/immunodynamic modelling methods in a proof of concept study.

Methods: Data on IFN-γ secreting CD4+ T cells over time after recent BCG vaccination were available for 55 humans and 81 macaques. Human population covariates were: baseline BCG vaccination status, time since BCG vaccination, gender and monocyte/lymphocyte cell count ratio. The macaque population covariate was colony of origin. A two-compartment mathematical model describing the dynamics of the post-BCG IFN-γ T cell response was calibrated to these data using nonlinear mixed effects methods. The model was calibrated to macaque and human data separately. The association between subpopulations and BCG immune response in each species was assessed. Which macaque subpopulations best predicted immune responses in different human subpopulations was identified using Bayesian Information Criteria.

Results: Macaque colony and human baseline-BCG status were significantly ($p<0.05$) associated with BCG-induced immune response. For baseline-BCG-naïve humans, Indonesian cynomolgus macaques and Indian rhesus macaques best predicted immune response. For baseline-BCG-vaccinated humans, Mauritian cynomolgus macaques best predicted immune response.

Conclusion: The work suggests that the immune responses of different human populations may be best modelled by different macaque colonies, and demonstrates the potential utility of immunostimulation/immunodynamic modelling to accelerate TB vaccine development.

41 **Introduction**

42

43 Tuberculosis (TB) disease remains a major global health problem (1) and Bacillus Calmette–Guérin
44 (BCG), the only licensed TB vaccine, exhibits variable efficacy (2, 3). A new, effective vaccine is vital
45 to reach WHO TB control goals (4). Animal models are used in almost every aspect of vaccine
46 development including helping to understand the transmission dynamics of the disease to the
47 immunogenicity and efficacy of a vaccine (5). They are therefore a vital and efficient tool in vaccine
48 development (6). In pre-clinical TB vaccine research, non-human primates (NHPs) are a valuable
49 animal model (7, 8), and are genetically and physiologically more similar to humans than small
50 animals with respect to TB disease and immune response (7, 9).

51 Historically, rhesus (*Macaca mulatta*) (10) and cynomolgus (*Macaca fascicularis*) (11) macaque
52 species have been used as the primary NHP-model in TB vaccine research (12-14). Both species have
53 been shown to respond to, and be partially protected from, TB by BCG vaccination (15-19); however,
54 it has been shown that the same experimental conditions (infection with *Mycobacterium*
55 *tuberculosis* (*Mtb*) following vaccination or vaccine immune response) may lead to divergent
56 outcomes between the two species (7, 20-22). Furthermore, the colony (country of origin) of
57 macaque, even within the same species, has been shown to affect the level of protection to infection
58 and response after vaccination. For example, differing levels of protection between Chinese and
59 Mauritian cynomolgus macaques have been observed, whereby Mauritian cynomolgus macaques
60 developed end stage progressive TB in 7 weeks, while the Chinese cynomolgus macaques remained
61 well past the end of the study (12 weeks)(23).

62 These differences suggest that the immune responses of different human populations (e.g. those
63 with previous BCG vaccination or those who are BCG-naïve) may be best modelled by different
64 macaque colonies. In 2014, the Bill and Melinda Gates Foundation adopted a new strategy for the
65 up-selection of new TB vaccine candidates for clinical testing selecting vaccines on immune response

and challenge results in NHPs (24). Therefore, it is critical that differences between macaque populations are identified and understood to increase the likelihood of developing an effective vaccine.

Here we focus on establishing the most representative NHP-model for modelling the human IFN-γ immune responses in UK adults following recent BCG vaccination, as one example of predicting vaccine immune response in humans from a macaque animal model.

To do this, we conduct a proof-of-concept study to evaluate the potential use of novel immunostimulation/immunodynamic (IS/ID) modelling methods in vaccine immune response translation between species. A mechanistic mathematical-based approach is used to quantify the dynamics of the immune response. By building the mathematical models based on the quantitative immunological data, it is possible to describe how these mechanisms may vary within and between species, and draw quantitative comparisons. Such modelling techniques are common in drug development (pharmacokinetic/pharmacodynamic modelling) to translate drug responses between species (25-27), but have yet to be used in vaccine development.

Firstly, we develop a model of post-BCG vaccination, IFN-γ producing CD4+ T cell dynamics, and assess the suitability of the model structure to predict responses by calibrating to data (analysis 1). We investigate the impact of the human and macaque population covariates to explain the within-population variation in responses, which our previous analysis on humans (28) showed can have a substantial impact on the magnitude of response (analysis 2). We then test which calibrated macaque models best predict human IFN-γ response (analysis 3). Finally, we use the calibrated mathematical models for macaque and human subpopulations to predict the dynamics of the constituent T cell populations over time (analysis 4).

88 **Methods**

89 Data

90

91 Data on the number of Purified Protein Derivative (PPD) stimulated CD4+ T-cells secreting IFN-γ (in
92 spot forming units (SFU)) per 1 million Peripheral Blood Mononuclear Cells (PBMC) measured by an
93 *ex vivo* IFN-γ Enzyme-Linked ImmunoSpot (ELISPOT) assay were available for 55 humans and 81
94 macaques. BCG vaccination was given on day 0 and ELISPOT measures were performed up to 140
95 days after vaccination. The details of the human dataset and laboratory techniques have been
96 published previously (28). Briefly, healthy UK volunteers aged 18-55, with no history of BCG
97 vaccination or previously immunised with BCG, were given 100 µl of BCG administered intradermally
98 in upper arm. Immune responses to BCG were measured using an IFN-γ ELISPOT assay at weeks 1, 4,
99 8 and 24. For demographics and laboratory detail see the supplementary material (Table S1, Figure
100 S1). All macaque studies were conducted in accordance with the Home Office (UK) Code of Practice
101 for the Housing and Care of Animals Used in Scientific Procedures (1989), and the National
102 Committee for Refinement, Reduction and Replacement (NC3Rs), Guidelines on Primate
103 Accommodation, Care and Use, August 2006 (NC3Rs, 2006). All animal procedures were approved by
104 the Public Health England, Porton Down Ethical Review Committee, and authorised under an
105 appropriate UK Home Office project license. Vaccination, sample collection procedures, and
106 immunological methods are described in full in (19, 23, 29, 30). All macaques were demonstrated to
107 be mycobacterially naïve prior to BCG vaccination and between 3 and 14 years old. The human
108 population covariates were: baseline (before vaccination at time 0) BCG vaccination status (either
109 baseline-BCG-vaccinated (BCG:Y) or baseline-BCG-naïve (BCG:N)); years since BCG vaccination
110 (groups were 1 to 9, 10 to 19, 20 to 29 years and "never"); gender; and monocyte to lymphocyte cell
111 count ratio (ML ratio). The macaque population covariate was colony of origin (rhesus: Indian,
112 cynomolgus: Chinese, cynomolgus: Mauritian and cynomolgus: Indonesian, see Table S2, Figure S2).
113 Rhesus macaques and Indonesian and Mauritian genotype cynomolgus macaques were obtained

from established UK breeding colonies. Chinese cynomolgus macaques were imported from a Home Office approved breeding colony in China.

Mathematical Immunostimulation/Immunodynamic (IS/ID) Model

An ordinary differential equations model was used to describe the IFN-γ response dynamics of two CD4+ T cell populations: transitional effector memory (31) and resting "central" memory, which are short and long-lived, respectively (32-34) (Figure 1). Briefly, cells were recruited into the transitional effector memory compartment at rate δ. A proportion, p of transitional effector memory cells apoptosed at rate μ_{TEM} and the remaining proportion (1-p) transitioned to central memory phenotype where they stayed for the duration of the model run (170 days) (Figure 1). Central memory cells are quiescent in the host until stimulated by antigen (35), however we considered them here to contribute to IFN-γ production as the ELISPOT assay uses PPD to stimulate all potentially IFN-γ secreting CD4+ T-cells. To reflect this, the IFN-γ immune response predicted by the mathematical model was the sum of the number of transitional effector memory and central memory cells populations over time. We assumed any non-zero responses at baseline to be an existing memory response that had immediately reverted to transitional effector memory phenotype in the presence of antigen. Therefore, the initial transitional effector memory population (TEM_0) was positive for those subjects. We assumed that the increase in the number of transitional effector memory and central memory cells did not occur immediately after vaccination, but gradually increased over time due to immune processes such as vaccine antigen trafficking and presentation (35, 36). It then subsided as T cell stimulation was assumed not to last indefinitely (35-39). The recruitment of transitional effector memory cells over time was controlled in the model using the recruitment rate, δ, which was a peaked curve specified using a gamma probability density function (PDF) distribution with parameters L, k and h (Figure 1).

138 Analyses

139

140 Analysis 1: Model calibration to IFN-γ data and exploration of model predictions for macaque and
141 humans, separately

142 In analysis 1, the model was calibrated to the macaque and human data separately to quantify the
143 dynamics of the IFN-γ response for each species. To do this, three parameters were estimated (the
144 components of function δ: L, k and h (Figure 1)) and, TEM_0, the initial number of transitional effector
145 memory cells using the established method of nonlinear mixed effects modelling (NLMEM) (40)
146 using the software *Monolix* v. 4.3.3 (41). Briefly, NLMEM uses maximum likelihood methods to
147 estimate the model parameters that best describe the population mean response and the associated
148 parameter variance which accounts for the within-population variation (for more details see (42)).
149 Evaluation of the model's ability to describe the data was conducted primarily by simulation based,
150 visual predictive check (VPC) plots (see supplementary methods for details); assessment of the
151 precision of the estimated parameters using the relative standard error (RSE) and a goodness of fit
152 measure (Bayesian Information Criteria (BIC)). A difference in BIC of >6 was considered a significant
153 (p-value< 0.05) effect (43) and a parameter RSE< 30% was considered a well estimated parameter.
154 The proportion of transitional effector memory cells that die (p) was assumed to be 0.925, as
155 supported by literature (33) (Figure 1, Table 1) and the parameter governing the mortality rate of
156 transitional effector memory cells, μ_E, was fixed after a scenario analysis was conducted (Table S3).
157 Further tests required to establish the NLMEM framework are outlined in Tables S4-S6.

158 Analysis 2: Population covariate impact on within-population variation in model parameter
159 estimates

160 In analysis 2, we explored whether population covariates (i.e. subpopulations e.g. such as colony)
161 could reduce the within-population variation of the estimated parameters from analysis 1, and thus

established a subpopulation-model for macaques and humans, separately. To do this, covariate-parameter relationships were tested and selected based a forward-addition strategy and likelihood ratio test method (see supplementary methods for details). Once the appropriate covariate-parameter relationship was found, the subpopulation-model was then calibrated to the data and the subpopulation parameters estimated. We observed the change in the BIC and within-population variation of model parameters from analysis 1 to analysis 2 as a result of accounting for the population covariates.

Analysis 3: Which macaque subpopulations best predicted immune responses in different human subpopulations?

To evaluate which macaque subpopulation best predicted the immune response in different human subpopulations, estimated parameters and parameter variances from the macaque subpopulation-model (analysis 2) and were fit to the human data (or human subpopulation data (analysis 2)). The subpopulation of macaque which best described the human data was defined as the model with the lowest BIC.

Analysis 4: Predicted number of transitional effector memory (TEM) and resting central memory (CM) cells over time

The calibrated mathematical model was then used to predict the number of transitional effector memory(31)(31) and resting central memory cells over time. These dynamics were not measured empirically.

Clinical and Vaccine Immunology

Results

Analysis 1: Model calibration to IFN-γ data and exploration of model predictions for macaque and humans, separately

The estimated parameter values for both species can be found in Table 1. The Visual Predictive Check (VPC) plot in Figure 2 shows the model simulated ranges for macaques and humans cover the empirical data, indicating our model is good representation of the empirical data. Further diagnostic plots and model prediction plots can be found in Figures S3-S7.

Analysis 2: Population covariate impact on within-population variation in model parameter estimates

We found two covariates to be important: stratifying macaques by colony and humans by baseline BCG status reduced the within-population variation in the macaque initial transitional effector memory cell count (TEM_0), the human initial transitional effector memory cell count, and the human gamma PDF multiplier and scale parameters (parameters L and h) (Table 1, S7-S13, Figures S8-S12). The VPC and further diagnostic plots for the subpopulation-models show the model describes the data adequately (Figures S13-S18). Accounting for the population covariates reduced the BIC value significantly by 73 in humans compared to analysis 1 (from BIC=2779 in analysis 1 to BIC=2706 in analysis 2, Table 1) and was decreased by 2 in macaques (from BIC=7253 in analysis 1 to BIC=7251 in analysis 2, Table 1). The model-predicted total mean number of IFN-γ secreting cells (transitional effector memory plus central memory cells) over time is shown in Figure 3 as a visual assessment of the goodness of model fit to the mean empirical data. Also, Figures S19 and S20 show the 10^{th} to 90^{th} percentiles of model predictions after accounting for within-population variation.

Analysis 3: Which macaque subpopulations best predicted immune responses in different human subpopulations?

The calibrated model for the Indonesian cynomolgus macaques from analysis 2, provided the lowest BIC values for the human BCG: N population, the Indian rhesus macaques provided the second lowest value (BIC values 1357 and 1391 respectively, Figures 4, S20-S27). The calibrated model for the Mauritian cynomolgus macaques best represented the BCG: Y humans (BIC value 1608, Figures 4, S21-S28).

Analysis 4: Predicted number of transitional effector memory (TEM) and resting central memory (CM) cells over time.

Figure 5 shows the model predicted number of total, transitional effector memory and central memory cells secreting IFN-γ, over time, for the mean macaque and human subpopulation data. These model dynamics present a prediction for the CD4+ T cell phenotypic behaviour, and how they differ between species and subpopulations, which could be validated experimentally.

Discussion

In our proof-of-concept study, we applied novel immunostimulation/immunodynamic (IS/ID) modelling to BCG immune response data and found that macaque colony and human baseline-BCG status were significantly ($p<0.05$) associated with BCG induced IFN-γ immune response. No other population covariates were significantly associated. For baseline-BCG-naïve humans, Indonesian cynomolgus macaques and Indian Rhesus macaques best predicted immune response. For baseline-BCG-vaccinated humans, Mauritian cynomolgus macaques best predicted immune response.

A key strength of this proof-of-concept study was the application of mathematical modelling techniques to vaccine data that are rarely explored quantitatively. We used established robust quantitative and statistical frameworks (compartmental mathematical models with NLMEM (40)) to explore the complex biological dynamics, giving an early example of the utility of IS/ID modelling. The biological data we used were standardised between species, with respect to time points and laboratory techniques, which allowed a direct comparison of the immune response to BCG vaccination.

Although our model was a highly simplified version of the complexities of the immune system (see supplementary discussion for main assumptions and their impact (Table S14)), analysis 1 showed the model described the data well. When applied to the subpopulation data in analysis 2, the IS/ID model was also a good description of the data. However, when calibrated to smaller subpopulation sizes (especially for the Chinese and Indonesian cynomolgus macaques) the estimated model parameters were more uncertain than for the larger populations (see relative standard error values in Table 1). Access to larger data sets on these populations would increase the certainty of the parameter estimates. Additionally, in analysis 2, our aim was to establish how population covariates affect the model parameters using a stepwise addition method. However, as Whittingham et al point out, despite is widespread use, there are inherent drawbacks with such a method (44).

By modelling the recruitment rate of transitional effector memory cells by the function δ, we were able to represent the nonlinear stimulation of the CD4 T cell response following BCG vaccination allowing comparison of the dynamics of the response between subpopulations. However, as the recruitment rate of transitional effector memory cells was not based on biological data and characterised by a theoretical shape, it is difficult to make direct biological interpretations of the parameters. To incorporate a mechanistic stimulation curve in future work, data on the cells involved in the stimulation response would be required.

The results in this analysis were consistent with previous work, in which we applied descriptive statistics to the human data (28). In that study, men experienced a higher baseline IFN-γ response (p-value<0.1) in comparison with women. A similar pattern can be seen in the current work as the median initial number of transitional effector memory cells (TEM_0) for men being higher than that of women (Figure S8). Additionally, the model in analysis 2 is consistent with (28) for humans, in which immune responses were higher in magnitude and sustained for longer for baseline-BCG-vaccinated humans than for baseline-BCG-naive humans. Therefore, our results suggest BCG revaccination provides a higher and more sustained IFN-γ response than primary vaccination in humans. Finally, our results suggest that there are differences in BCG response between the colonies of macaques. This is consistent with work by Langermans et al., who show that rhesus macaques experience higher IFN-γ response 13 weeks after BCG vaccination than cynomolgus macaques (22), although the potential effect of colony on IFN-γ response was not highlighted in that work. Differences in responses across macaque colony are also true in *Mtb* challenge studies: Sharpe et al. showed that IFN-γ secreting CD4 T cells AUC_{12Week} values were significantly higher for Indian rhesus macaques than Indonesian cynomolgus (21). Although we don't consider *Mtb.* challenge in our analysis, these differences may be important to consider when selecting an NHP model for human mycobacterial immune response.

Our results imply that responses in Indonesian cynomolgus macaques followed by Indian rhesus macaques most closely resembled the ELISPOT response in primary vaccinated humans. However, we approach this conclusion with caution, as the sample sizes of the macaque colony subpopulations were variable. With these smaller sample sizes model parameterization and validation are less reliable than for the larger groups. More data on the colonies with small sample sizes should be collected and re-modelled to verify our results. Nevertheless, the large sample size obtained for the Indian rhesus macaques was collated over decades of experimentation. Conventional vaccine studies in macaques are often limited to 6-9 per group due to space and cost. These smaller macaque experiments are then used to inform clinical vaccine trials, making our small sample sizes more representative of current vaccine development.

It is important to note that, in terms of BCG vaccination history, this human subpopulation is the most comparable to all of the macaque subpopulations. Mauritian cynomolgus macaques made the highest response to a primary BCG vaccination and therefore most closely resemble revaccination in humans. However, it is apparent from Figure 4 that the BCG vaccinated humans experienced a considerably higher magnitude of responses than all of the macaque (baseline-BCG-naïve) subpopulations. This suggests that the immune response to an antigen encountered for the first time is lower and slower than the response induced to the same antigen on subsequent occasions (35). Our results, therefore suggest that a revaccinated macaque animal model for revaccinated humans may be most appropriate. This should be considered in further IS/ID translational analysis between macaques and humans.

In our analyses, we only consider a UK-based human population. In future evaluations, a similar analysis to that presented here could be carried out on populations from varying geographical locations, as BCG responses have been shown to vary by geographic location (45). Other population covariates, such as age may also be important (8). Additionally, whether this analysis will be similar for other candidate vaccines would benefit from further scrutiny.

Figure 5 explored the dynamics of the constituent T cell populations, and provided insights into how and when memory may be developed - an important consideration in vaccine regimen design, i.e. timing of revaccination and if varies between subpopulations. However, we do not currently have data to support these dynamics, so future work could be undertaken using flow cytometry to characterise the relative number of complex phenotypic cell types over time and thus inform models that can provide better understanding of T-cell dynamics.

In this analysis, we used solely IFN-γ as an proxy for BCG vaccine immunogenicity (46) and do not consider BCG efficacy measures explicitly. We appreciate that in order to develop a vaccine, both immunogenicity and efficacy are vital considerations. Therefore, in predicting which macaque model best represents the human vaccine response, vaccine efficacy cannot be ignored. However, to incorporate efficacy would require more complex models and data than we present here. As more immunological information or functional parameters becomes available, IS/ID modelling methods allow us to easily integrate new information, e.g. on cytokines, cells or for efficacy measures, bacteria counts. Thus, we would be able to make decisions on the best NHP model to use based on a more complete vaccine performance framework.

Conclusion

This work suggests that the immune responses of different human subpopulations may be best modelled by different macaque colonies, and demonstrates the potential utility of immunostimulation/immunodynamic modelling to TB accelerate vaccine development.

Acknowledgements

We would like to thank our colleagues at INSERM (J. Guedj and F. Mentre), Paris who provided training into the NLMEM methods.

Funding

SR is supported by a LSHTM studentship funded by Aeras. GK is funded by the National Institute for Health Research Health Protection Research Unit (NIHR HPRU) in Healthcare Associated Infection and Antimicrobial Resistance at Imperial College London in partnership with Public Health England (PHE). The views expressed are those of the author(s) and not necessarily those of the NHS, the NIHR, the Department of Health or Public Health England. RGW is funded the UK Medical Research Council (MRC) and the UK Department for International Development (DFID) under the MRC/DFID Concordat agreement that is also part of the EDCTP2 programme supported by the European Union (MR/P002404/1), the Bill and Melinda Gates Foundation (TB Modelling and Analysis Consortium: OPP1084276/OPP1135288, SA Modelling for Policy: OPP1110334, CORTIS: OPP1137034, Vaccines: OPP1160830) and UNITAID (4214-LSHTM-Sept15; PO 8477-0-600).

Competing Financial Interest

The author(s) declare no competing financial interests.

References

1. **WHO.** 2015. Global Tuberculosis Report 2015. World Health Organization, WHO,
2. **Mangtani P, Abubakar I, Ariti C, Beynon R, Pimpin L, Fine PE, Rodrigues LC, Smith PG, Lipman M, Whiting PF, Sterne JA.** 2014. Protection by BCG vaccine against tuberculosis: a systematic review of randomized controlled trials. Clin Infect Dis **58:**470-480.
3. **Dye C.** 2013. Making wider use of the world's most widely used vaccine: Bacille Calmette-Guerin revaccination reconsidered. J R Soc Interface **10:**20130365.
4. **Dye C, Glaziou P, Floyd K, Raviglione M.** 2013. Prospects for tuberculosis elimination. Annu Rev Public Health **34:**271-286.
5. **Acosta A, Norazmi MN, Hernandez-Pando R, Alvarez N, Borrero R, Infante JF, Sarmiento ME.** 2011. The importance of animal models in tuberculosis vaccine development. Malays J Med Sci **18:**5-12.
6. **Tanner R, McShane H.** 2016. Replacing, reducing and refining the use of animals in tuberculosis vaccine research. ALTEX doi:10.14573/altex.1607281.
7. **Flynn JL, Gideon HP, Mattila JT, Lin PL.** 2015. Immunology studies in non-human primate models of tuberculosis. Immunol Rev **264:**60-73.
8. **McShane H, Williams A.** 2014. A review of preclinical animal models utilised for TB vaccine evaluation in the context of recent human efficacy data. Tuberculosis (Edinb) **94:**105-110.
9. **Carlsson HE, Schapiro SJ, Farah I, Hau J.** 2004. Use of primates in research: a global overview. Am J Primatol **63:**225-237.
10. **Gormus BJ, Blanchard JL, Alvarez XH, Didier PJ.** 2004. Evidence for a rhesus monkey model of asymptomatic tuberculosis. J Med Primatol **33:**134-145.
11. **Capuano SV, 3rd, Croix DA, Pawar S, Zinovik A, Myers A, Lin PL, Bissel S, Fuhrman C, Klein E, Flynn JL.** 2003. Experimental Mycobacterium tuberculosis infection of cynomolgus macaques closely resembles the various manifestations of human M. tuberculosis infection. Infect Immun **71:**5831-5844.
12. **Pena JC, Ho WZ.** 2015. Monkey models of tuberculosis: lessons learned. Infect Immun **83:**852-862.
13. **Kaushal D, Mehra S, Didier PJ, Lackner AA.** 2012. The non-human primate model of tuberculosis. J Med Primatol **41:**191-201.
14. **Scanga CA, Flynn JL.** 2014. Modeling tuberculosis in nonhuman primates. Cold Spring Harb Perspect Med **4:**a018564.
15. **Barclay WR, Anacker RL, Brehmer W, Leif W, Ribi E.** 1970. Aerosol-Induced Tuberculosis in Subhuman Primates and the Course of the Disease After Intravenous BCG Vaccination. Infect Immun **2:**574-582.
16. **Janicki BW, Good RC, Minden P, Affronti LF, Hymes WF.** 1973. Immune responses in rhesus monkeys after bacillus Calmette-Guerin vaccination and aerosol challenge with Mycobacterium tuberculosis. Am Rev Respir Dis **107:**359-366.
17. **Reed SG, Coler RN, Dalemans W, Tan EV, DeLa Cruz EC, Basaraba RJ, Orme IM, Skeiky YA, Alderson MR, Cowgill KD, Prieels JP, Abalos RM, Dubois MC, Cohen J, Mettens P, Lobet Y.** 2009. Defined tuberculosis vaccine, Mtb72F/AS02A, evidence of protection in cynomolgus monkeys. Proc Natl Acad Sci U S A **106:**2301-2306.
18. **Kaushal D, Foreman TW, Gautam US, Alvarez X, Adekambi T, Rangel-Moreno J, Golden NA, Johnson AM, Phillips BL, Ahsan MH, Russell-Lodrigue KE, Doyle LA, Roy CJ, Didier PJ, Blanchard JL, Rengarajan J, Lackner AA, Khader SA, Mehra S.** 2015. Mucosal vaccination

Clinical and Vaccine Immunology

with attenuated Mycobacterium tuberculosis induces strong central memory responses and protects against tuberculosis. Nat Commun **6:**8533.

19. **White AD, Sarfas C, West K, Sibley LS, Wareham AS, Clark S, Dennis MJ, Williams A, Marsh PD, Sharpe SA.** 2015. Evaluation of the Immunogenicity of Mycobacterium bovis BCG Delivered by Aerosol to the Lungs of Macaques. Clin Vaccine Immunol **22:**992-1003.
20. **Sharpe SA, Eschelbach E, Basaraba RJ, Gleeson F, Hall GA, McIntyre A, Williams A, Kraft SL, Clark S, Gooch K, Hatch G, Orme IM, Marsh PD, Dennis MJ.** 2009. Determination of lesion volume by MRI and stereology in a macaque model of tuberculosis. Tuberculosis (Edinb) **89:**405-416.
21. **Sharpe S, White A, Gleeson F, McIntyre A, Smyth D, Clark S, Sarfas C, Laddy D, Rayner E, Hall G, Williams A, Dennis M.** 2016. Ultra low dose aerosol challenge with Mycobacterium tuberculosis leads to divergent outcomes in rhesus and cynomolgus macaques. Tuberculosis (Edinb) **96:**1-12.
22. **Langermans JA, Andersen P, van Soolingen D, Vervenne RA, Frost PA, van der Laan T, van Pinxteren LA, van den Hombergh J, Kroon S, Peekel I, Florquin S, Thomas AW.** 2001. Divergent effect of bacillus Calmette-Guerin (BCG) vaccination on Mycobacterium tuberculosis infection in highly related macaque species: implications for primate models in tuberculosis vaccine research. Proc Natl Acad Sci U S A **98:**11497-11502.
23. **Javed S, Marsay L, Wareham A, Lewandowski KS, Williams A, Dennis MJ, Sharpe S, Vipond R, Silman N, Ball G, Kempsell KE.** 2016. Temporal Expression of Peripheral Blood Leukocyte Biomarkers in a Macaca fascicularis Infection Model of Tuberculosis; Comparison with Human Datasets and Analysis with Parametric/Non-parametric Tools for Improved Diagnostic Biomarker Identification. PLoS One **11:**e0154320.
24. **Hanekom W, Johnston P, Kaplan G, Karp C, Shackelton L, Stuart L, Wilson C.** 2014. Revision of the Bill & Melinda Gates Foundation TB vaccine strategy - 2014.
25. **Knibbe CA, Zuideveld KP, Aarts LP, Kuks PF, Danhof M.** 2005. Allometric relationships between the pharmacokinetics of propofol in rats, children and adults. Br J Clin Pharmacol **59:**705-711.
26. **Dubois VF, de Witte WE, Visser SA, Danhof M, Della Pasqua O, Cardiovascular Safety Project T, Platform TIPP.** 2016. Assessment of Interspecies Differences in Drug-Induced QTc Interval Prolongation in Cynomolgus Monkeys, Dogs and Humans. Pharm Res **33:**40-51.
27. **Mould DR, Upton RN.** 2012. Basic concepts in population modeling, simulation, and model-based drug development. CPT Pharmacometrics Syst Pharmacol **1:**e6.
28. **Rhodes SJ, Knight GM, Fielding K, Scriba TJ, Pathan AA, McShane H, Fletcher H, White RG.** 2016. Individual-level factors associated with variation in mycobacterial-specific immune response: Gender and previous BCG vaccination status. Tuberculosis (Edinb) **96:**37-43.
29. **White AD, Sibley L, Dennis MJ, Gooch K, Betts G, Edwards N, Reyes-Sandoval A, Carroll MW, Williams A, Marsh PD, McShane H, Sharpe SA.** 2013. Evaluation of the safety and immunogenicity of a candidate tuberculosis vaccine, MVA85A, delivered by aerosol to the lungs of macaques. Clin Vaccine Immunol **20:**663-672.
30. **Sharpe SA, McShane H, Dennis MJ, Basaraba RJ, Gleeson F, Hall G, McIntyre A, Gooch K, Clark S, Beveridge NE, Nuth E, White A, Marriott A, Dowall S, Hill AV, Williams A, Marsh PD.** 2010. Establishment of an aerosol challenge model of tuberculosis in rhesus macaques and an evaluation of endpoints for vaccine testing. Clin Vaccine Immunol **17:**1170-1182.
31. **Seder RA, Darrah PA, Roederer M.** 2008. T-cell quality in memory and protection: implications for vaccine design. Nat Rev Immunol **8:**247-258.
32. **Pepper M, Jenkins MK.** 2011. Origins of CD4(+) effector and central memory T cells. Nat Immunol **12:**467-471.
33. **Kaech SM, Wherry EJ, Ahmed R.** 2002. Effector and memory T-cell differentiation: implications for vaccine development. Nat Rev Immunol **2:**251-262.

34. **McKinstry KK, Strutt TM, Swain SL.** 2010. The potential of CD4 T-cell memory. Immunology **130:**1-9.
35. **Abbas A, Lichtman A, Pillai S.** 2015. Cellular and Molecular Immunology, 8 ed. Elsevier Saunders.
36. **Urdahl KB, Shafiani S, Ernst JD.** 2011. Initiation and regulation of T-cell responses in tuberculosis. Mucosal Immunol **4:**288-293.
37. **Chackerian AA, Alt JM, Perera TV, Dascher CC, Behar SM.** 2002. Dissemination of Mycobacterium tuberculosis is influenced by host factors and precedes the initiation of T-cell immunity. Infect Immun **70:**4501-4509.
38. **Cooper AM.** 2009. Cell-mediated immune responses in tuberculosis. Annu Rev Immunol **27:**393-422.
39. **De Rosa SC.** 2004. Multicolor immunophenotyping: human mature immune system. Methods Cell Biol **75:**577-594.
40. **Lavielle M.** 2015. Mixed Effects Models for the Population Approach: Models, Tasks, Methods and Tools. Chapman & Hall.
41. **Anonymous.** 2014. Monolix: Users Guide, v4.3.3. http://www.lixoft.eu/.
42. **Lavielle M, Mentre F.** 2007. Estimation of population pharmacokinetic parameters of saquinavir in HIV patients with the MONOLIX software. J Pharmacokinet Pharmacodyn **34:**229-249.
43. **Raftery A.** 1995. Bayesian Model Selection in Social Research. Sociological Methodology **25:**111-163.
44. **Whittingham MJ, Stephens PA, Bradbury RB, Freckleton RP.** 2006. Why do we still use stepwise modelling in ecology and behaviour? Journal of Animal Ecology **75:**1182 - 1189.
45. **Weir RE, Black GF, Nazareth B, Floyd S, Stenson S, Stanley C, Branson K, Sichali L, Chaguluka SD, Donovan L, Crampin AC, Fine PE, Dockrell HM.** 2006. The influence of previous exposure to environmental mycobacteria on the interferon-gamma response to bacille Calmette-Guerin vaccination in southern England and northern Malawi. Clin Exp Immunol **146:**390-399.
46. **Fletcher HA.** 2007. Correlates of immune protection from tuberculosis. Curr Mol Med **7:**319-325.

Figure 1: Schematic of A) the mathematical model representing the immune response dynamics of two CD4+ T cell populations secreting IFN-γ, B) depiction of how the recruitment rate of transitional effector memory cells (δ) changes over time and C) key model parameters. Equations can be found in the supplementary material.

Figure 2 : Visual Predictive Check (VPC) plot showing number of IFN-γ SFU/million PMBC, by time (days) for A) all macaques and B) all humans. The VPC plot assesses the appropriateness of the proposed mathematical model (Figure 1) to describe the empirical data by comparing data simulated using the model and population mean parameters and associated variances (Table 1), to the empirical data distribution (see supplementary methods for more detail). Blue points show empirical data. Pink regions represents the range of the medians of the simulated data for 500 simulations. Blue regions represent the ranges of the 90th and 10th percentiles of the simulated population data. The green line links the empirical percentiles (10th, 50th and 90th). Dark red regions represent where the empirical data falls outside the ranges of the simulated percentiles. The lack of dark red regions (aside from where data are variable between time points in macaques) indicates our proposed mathematical model (Figure 1) adequately represents the empirical data.

Figure 3: Data (black points) and model predicted (black lines) total number of T cells secreting IFN-γ (sum of the number of Transitional effector memory cells and resting central memory cells), over time. Model predictions use the estimated subpopulation-model parameters from Table 1 for the four macaque colonies and the two human BCG status subpopulations. Points represent the mean of the data at each time point. (NB note the scale differences for human).

Figure 4: Data (black Points and red triangles) and model predicted (lines) mean immune responses for the four macaque colonies and human BCG: Y (left) and BCG: N (right) with the human empirical responses and mean empirical responses. The tables show the results of assessing the ability of the calibrated macaque colony mathematical model parameters (analysis 2, Table 1) to describe the human data for BCG: Y and BCG: N subpopulations. *BIC values are in ranked order, lowest to highest and all difference in BIC are significant (difference in BIC>6 (43)). Abbreviations: BCG: Y = those human participants who were baseline-BCG-vaccinated, BCG: N = human participants who were baseline-BCG-naïve, cyn. = cynomolgus, BIC = Bayesian Information Criteria.

Figure 5: Data (black points), predicted total number of T cells secreting IFN-γ (black line), predicted number of transitional effector memory (TEM) cells (green line), and predicted number of resting central memory (CM) cells (orange line), over time. Model predictions use the estimated subpopulation-model parameters from Table 1 for the four macaque colonies and the two human BCG status subpopulations (NB note the scale differences for human).

	Macaque					Human				
	All (analysis 1)		Covariate (analysis 2)			All (analysis 1)		Covariate (analysis 2)		
Parameter (unit) (F=Fixed, E=Estimate)	**Value**	**RSE (%)**	**Subpop.**	**Value**	**RSE (%)**	**Value**	**RSE (%)**	**Subpop.**	**Value**	**RSE (%)**
Initial number of TEM cells (TEM_0) (cells) (E)	20.7	29	Chi	0.29	39*	59.9	17	BCG:Y	149	15
			Maur	65.1	24					
			Indo	23.2	41*			BCG:N	30.6	14
			R: Ind	15.7	20					
Gamma PDF curve multiplier (L) (scalar)(E)	1,170	13	Chi	617	43*	1490	14	BCG:Y	3240	14
			Maur	1,460	28					
			Indo	1,100	45*			BCG:N	747	14
			R: Ind	1,250	14					
Gamma PDF curve shape parameter (k) (scalar)(E)	3.31	5	Chi	4.3	11	1.45	9		1.55	16
			Maur	3.15	10					
			Indo	3	20					
			R: Ind	3.53	6					
Gamma PDF curve scale parameter (h) (scalar)(E)	15	8		13.8	7	18.4	18	BCG:Y	21.7	24
								BCG:N	15.2	34*
Initial number of CM cells (CM_0) (cells) (F)	0	-		0	-	0	-		0	-
TEM cell terminal mortality rate (μ_{TEM}) (/day) (F)	0.1	-		0.1	-	0.083	-		0.083	-
Proportion of TEM cells that die (p) (proportion) (F)	0.925	-		0.925	-	0.925	-		0.925	-
Within-population variation (WPV) (%)										
Initial TEM cell population (TEM_0)	130	25		41	27	107	15		52	19
Gamma PDF curve multiplier (L)	96	13		90	13	95	10		61	12
Gamma PDF curve shape parameter (k)	24	24		23	24	25	28		32	33*
Gamma PDF curve scale parameter (h)	19	21		21	20	58	25		43	37*
Goodness of fit statistics										
-2LL	7209			7183		2738			2653	
BIC	7253			7251		2779			2706	

Table 1 : Population mean parameter estimates for analysis 1 and 2 for macaques and humans. For details on the parameter-covariate relationship see supplementary methods. Abbreviations: TEM = transitional effector memory, CM = central memory, PDF = Probability Density Function, RSE = relative standard error, subpop. = subpopulation, Chi = Chinese cynomolgus macaques, Maur = Mauritian cynomolgus macaques, Indo = Indonesian cynomolgus macaques, R: Ind = Indian rhesus macaques,

Clinical and Vaccine Immunology

BCG: Y = those human participants who were baseline-BCG-vaccinated, BCG: N = human participants who were baseline-BCG-naïve; -2LL = -2*Log Likelihood. BIC = Bayesian Information Criteria; *: RSE >=30%.

Clinical and Vaccine Immunology

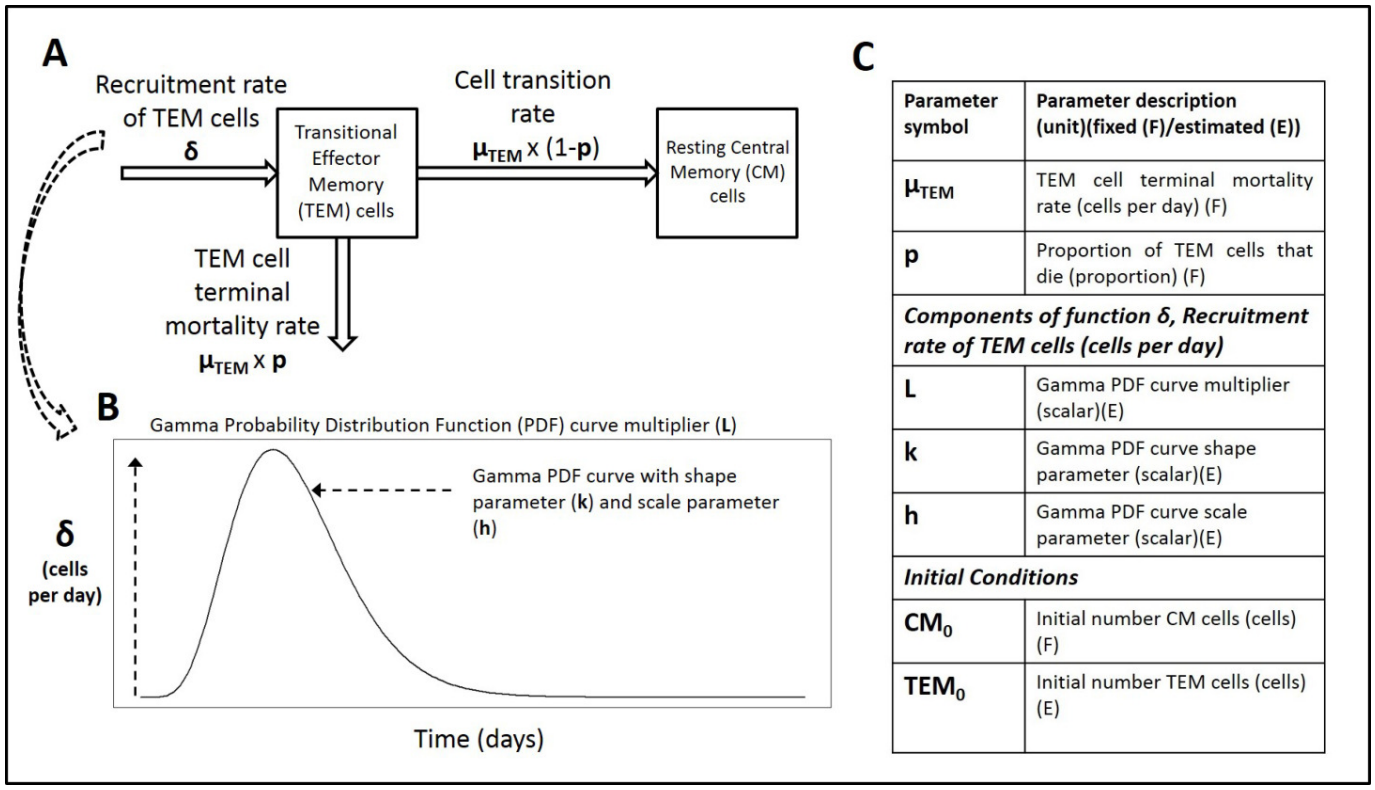

C

Parameter symbol	Parameter description (unit)(fixed (F)/estimated (E))
μ_{TEM}	TEM cell terminal mortality rate (cells per day) (F)
p	Proportion of TEM cells that die (proportion) (F)
Components of function δ, Recruitment rate of TEM cells (cells per day)	
L	Gamma PDF curve multiplier (scalar)(E)
k	Gamma PDF curve shape parameter (scalar)(E)
h	Gamma PDF curve scale parameter (scalar)(E)
Initial Conditions	
CM_0	Initial number CM cells (cells) (F)
TEM_0	Initial number TEM cells (cells) (E)

Clinical and Vaccine Immunology

Macaque subpopulation model fit to BCG: Y Data	
Colony	BIC value*
Mauritian cyn.	1608
Indonesian cyn.	2039
Indian rhesus	2056
Chinese cyn.	6589

Macaque subpopulation model fit to BCG: N Data	
Colony	BIC value*
Indonesian cyn.	1357
Indian rhesus	1391
Mauritian cyn.	1409
Chinese cyn.	2645